IEEE Access
Multidisciplinary ⋮ Rapid Review ⋮ Open Access Journal

Received 22 July 2022, accepted 8 August 2022, date of publication 18 August 2022, date of current version 29 August 2022.

Digital Object Identifier 10.1109/ACCESS.2022.3199697

RESEARCH ARTICLE

Resilient Adaptive Event-Triggered Control for Singular Networked Cascade Control Systems Under DoS Attacks

M. SATHISHKUMAR, (Member, IEEE), AND YEN-CHEN LIU, (Senior Member, IEEE)
Department of Mechanical Engineering, National Cheng Kung University, Tainan 70101, Taiwan

Corresponding author: Yen-Chen Liu (yliu@mail.ncku.edu.tw)

This work was supported in part by the Ministry of Science and Technology, Taiwan, under Grant MOST 111-2636-E-006-004.

ABSTRACT This paper addresses the problem of resilient adaptive event-triggered control for singular networked cascade control systems (SNCCSs) under time-varying actuator faults, actuator saturation, DoS attacks, external disturbances, and time-varying delay. The purpose of DoS attacks is to obstruct network communication from time to time, which happens aperiodically. According to the adaptive threshold technique, a resilient adaptive event-triggered mechanism (AETM) is developed to reduce the transmission frequency and also combating the aperiodic DoS attacks. Moreover, the discussed SNCCS is modeled as a switched system due to the presence of attacks that is closely restricted by DoS frequency and duration. Then, the exponential admissible analysis and controller synthesis conditions of the resulting switched SNCCS are obtained and the extended dissipative performance is satisfied by using the Wirtinger-based integral inequality and Lyapunov-Krasovskii functional (LKF) approach. Additionally, a co-design method of the primary and secondary controllers and triggering parameters for the system under consideration is given. Simulation results of a boiler-turbine power plant are presented to validate the proposed method.

INDEX TERMS Singular networked cascade control systems (SNCCSs), adaptive event-triggered (ET) control, actuator saturation, DoS attacks.

I. INTRODUCTION

In recent years, cascade control system has attracted significant attention from researchers due to its wide applicability in many engineering fields such as power plants, chemical reactors, and neural networks. Specifically, a pair of control loops is used in control algorithm, where the outer (secondary control) loop is embedded with inner (primary control) loop. In this algorithm, the outer loop is able to quickly eliminate disturbances, while the inner loop is responsible for the stability of the system. They have been successfully used to improve the performance of control systems in the face of disturbances, e.g., in networked control systems (NCSs) [1], [2], [3], [4]. The network in the control loop creates communication constraints due to the inherent limitation of the network bandwidth. Delay and dropout of data packets are two major problems known to cause instability or performance degradation in this type of control system [5], [6], [7]. Various techniques have been used for stability analysis of NCS considering these inherent characteristics [8], [9].

The open communication environment can expose many sensitive or private data to malicious attacks, which would lead to data unavailability and unreliability, even serious incidents or control performance degradation [10], [11], [12]. Most network communication-based attacks are categorized as replay attacks, deception attacks, and DoS attacks. Unlike replay attacks and deception attacks, DoS attacks use high traffic to disrupt their targets' communication links. Therefore, these types of attack models are not only less complicated, but also increasing the profit for the attackers due to their higher success rate in the network environment. These features make DoS attacks more often and useful [13], [14]. In [15], the authors discussed exponential stability and $\mathcal{L}_2$ performance issues for NCSs with DoS attacks and

The associate editor coordinating the review of this manuscript and approving it for publication was Feiqi Deng.

transmission delays under ET mechanism. Based on different DoS attack models in communication channels, ET predictive control was investigated in [16] to stabilize NCSs.

Singular systems have been extensively discussed and are also called differential algebraic or descriptive systems. The emerging field has attracted attention since they appear in a variety of domains, including mechanical systems, power systems, chemical processes, and electrical networks. Despite the fact that SNCCSs have many advantages, they inevitably introduce some crucial problems, such as exogenous disturbances, network-based attacks, unpredictable actuator faults, and time-varying delays, which pose a great challenge to the analysis and design of SNCCSs. For example, in [17], the authors discussed H_∞ control for SNCCSs with state delay. By introducing an ET H_∞ control, the authors reported stabilization and modelling problems for SNCCSs with constant delay in [18]. Hence, it is crucial to examine how to develop the performance requirements for SNCCSs under fundamental problems of network induced delays and DoS attacks. This is our initial motivation for this paper.

It should be noted that a large amount of data is generated during information transmission. As a result, a networked transmission channel's limited communication bandwidth increases network load and, to some extent, reduces transmission efficiency. For networked systems, solving the bandwidth limitation issue has always been an important issue. Currently, the ET scheme becomes a predominant approach to solving these issues. In contrast to the traditional time-triggered scheme, the ET scheme can decide whether to send the currently sampled data to the next control terminal when a predefined protocol is violated. This is an effective method for reducing the waste of computing resources and enhancing the efficiency of transmission [16], [19], [20] and the references therein. For example, the load frequency control was designed in [21] for interconnected multi-area power systems, where an ET scheme is used to reduce unwanted data transfers through the network. Nevertheless, the triggering conditions for the conventional ET scheme are almost static, i.e., the parameters for the triggering threshold are constant and cannot be dynamically adjusted to adapt to the effects of emergencies.

To overcome the conservative nature of constant parameters, some researchers have focused on a variable threshold AETM. The AETM was proposed in [22], with the trigger threshold parameter being a time-varying function that can be adjusted in real time according to the changes in the error dynamics. So far, some results based on the AETM have been reported [23]. In [24], an adaptive rule-based ET sliding mode control problem for stochastic systems under semi-Markov switching parameters was investigated. Adaptive dynamic program based control for nonlinear systems under DoS attacks was discussed in [25] using an adaptively adjusting ET mechanism. From another point of view, new methods for SNCCS have been proposed, in which H-infinity analysis is an effective method [17], [18]. The concept of extended dissipative analysis for Markov jump systems was developed in [26]. In addition, the new concept can be transformed into well-known performance indicators through the proper selection of the weighting matrix and the examples are dissipative, H-infinity, passive, and L_2-L_∞. As far as we know, extended dissipative and admissible analysis issues for SNCCSs with time-varying faults and aperiodic DoS attacks have not been studied yet, which highly inspired us to do this work.

Moreover, the problem of adaptive ET control with DoS attacks seems to be a challenging task with the following four main difficulties: *(1) In order to eliminate the effects of aperiodic DoS attacks, how do we design an appropriate AETM? (2) If information transmission is subject to DoS attacks, how to determine the next triggering instant for communication? (3) When communication is interrupted, how to update the control protocol? (4) How to reduce the number of trigger instants while achieving the desired system performance?*

In light of the discussion above, we investigate the problem of resilient adaptive ET control of SNCCSs with DoS attacks and actuator saturation in the current study. The overall contributions of this article can be given in the following aspects:

(1) In the admissible analysis of SNCCS, four important inherent attributes are considered simultaneously, including network based DoS attacks, actuator faults, network delays, and actuator saturation. Most of the published work addresses only one or two of these inherent attributes, while ignoring others [17], [18].
(2) Most of the existing results refer to periodic DoS attacks [20], [27], in the present study we deal with aperiodic DoS attacks, and the conditions developed for DoS duration and frequency are closer to the real situation.
(3) The AETM is designed to actively balance the negative impact of aperiodic DoS attacks. In contrast to conventional ET scheme, the method we have developed in this paper can result in a smaller amount of transmitted data. This can help to save more network bandwidth while guaranteeing the desired system performance.

In summary, the goal of the present work is to study the admissible analysis of SNCCSs while considering actuator faults, DoS attacks, delays, and actuator saturation simultaneously, which is much closer to the actual conditions. Here, the state-feedback controller is designed under AETM, which involves a number of LMIs. Finally, simulation results of a boiler-turbine power plant are presented to validate the proposed scheme.

II. PRELIMINARIES AND PROBLEM FORMULATION

In this paper, we consider a two-loop SNCCS, where the outer loop comprises the **Plant** Σ_1, **Sensor 1**, **Controller 1**, and **Actuator**, and the inner loop composes of the **Plant** Σ_2, **Sensor 2**, **Controller 2**, and **Actuator**. As given in FIGURE 1, the communication channels between **Sensor 1** and **Controller 1** in the primary control loop, and **Controller 2** and **Actuator** in the secondary control loop may be attacked by the malicious adversaries, that is, DoS attacks.

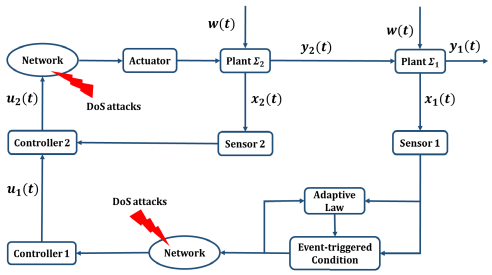

FIGURE 1. Structure of SNCCSs under AETM with DoS attacks.

The communication is not allowed when DoS threats are presented so that data cannot be successfully transmitted over the network. This means that the sampled state released by the AETM cannot be sent to **Controller 1** in the outer control loop, and the control signal transmitted by **Controller 2** cannot be transmitted to **Actuator** in the inner control loop. The following are the system description, DoS attacks, AETM, control protocol and the resulting switched system are presented, which are useful for understanding the problem.

A. SYSTEM DESCRIPTION

We consider the primary plant of NCCSs as

$$\Sigma_1: \begin{cases} \dot{x}_1(t) = A_1 x_1(t) + B_1 y_2(t), \\ y_1(t) = C_1 x_1(t) + D_1 w(t), \end{cases} \tag{1}$$

where $x_1(t)$ represents the state vector of the primary plant Σ_1; $y_1(t)$ denotes the output vector of the primary plant Σ_1; $y_2(t)$ represents the output vector of the secondary plant Σ_2. A_1, B_1, C_1 and D_1 denote the known constant matrices in the primary system (1) with suitable dimensions. By using the singular system, the secondary plant Σ_2 is modeled as

$$\Sigma_2: \begin{cases} E\dot{x}_2(t) = A_2 x_2(t) + A_3 x_2(t-\tau(t)) \\ +B_2 satu(u_2(t)) + B_3 w(t), \\ y_2(t) = C_2 x_2(t) + D_2 w(t), \\ x_2(t) = \phi(t), \quad t \in [-\tau_2, 0], \end{cases} \tag{2}$$

where $x_2(t)$, $u_2(t)$, $y_2(t)$ denote the state, control input, output vectors of the secondary plant Σ_2, respectively, and $w(t)$ is the exogenous disturbances. In (2), E represents the singular matrix that satisfies $rank(E) = r \leq n$. $A_2, A_3, B_2, B_3, C_2, D_2$ denote the appropriate known constant matrices. The initial condition of the function $\phi(t)$ is defined as $[-\tau_2, 0]$ and $\tau(t)$ implies the time-varying delay that satisfies $\tau(t) \in [0, \tau_2]$ with $\dot{\tau}(t) \leq \nu < \infty$, where ν is a positive integer. Moreover, $satu(u_2(t))$ denotes the saturation function, which is defined as $satu(u_2(t)) = \left[satu(u_2^1(t))\ satu(u_2^2(t)) \cdots satu(u_2^m(t))\right]^T \in \mathbb{R}^m$ with

$$satu(u_2^i(t)) = \begin{cases} \Psi_i, & u_2^i > \Psi_i, \\ u_2^i, & -\Psi_i \leq u_2^i \leq \Psi_i, \\ -\Psi_i, & u_2^i < -\Psi_i, \end{cases} \tag{3}$$

where Ψ_i $(i = 1, 2, \cdots, m)$ is the upper bound of (2) and is known. The saturation function $satu(u_2(t))$ is divided into a linear and a nonlinear function. Hence, we consider the following saturation model as

$$satu(u_2(t)) = u_2(t) - \Xi(u_2(t)). \tag{4}$$

In addition, $\Xi(u_2(t))$ denotes the dead-zone nonlinearity function and holds the below constraint that there exists $\epsilon \in (0, 1)$ with $\epsilon = \max\{\epsilon_1, \epsilon_2, \cdots, \epsilon_m\}$ such that

$$\epsilon u_2^T(t) u_2(t) \geq \Xi^T(u_2(t)) \Xi(u_2(t)). \tag{5}$$

B. ACTUATOR FAILURES

In this subsection, the following actuator fault model for the primary controller is developed as

$$u_{1,k}^{\aleph}(t) = (1 - \aleph_k(t)) u_{1,k}(t), \quad 0 \leq \aleph_k(t) \leq \bar{\aleph}_k < 1, \tag{6}$$

where, for $k = 1, 2, \cdots, m$ (denotes the kth actuator) and $u_{1,k}^{\aleph}(t)$ denotes the output signal from the primary actuator, $u_{1,k}$ represents the input signal of the primary actuator. $\aleph_k(t)$ is an unknown and piecewise continuous bounded failure factor of the primary actuator, indicating the degree of effectiveness of the primary actuator. The upper bound of $\aleph_k(t)$ is a known constant and is denoted by $\bar{\aleph}_k$. It noted that if $\aleph_k(t)$ is equal to zero, then the kth actuator is healthy or normal (i.e., no fault); when $0 < \aleph_k(t) < 1$, then the kth actuator is respect to loss of effectiveness fault (i.e., partially failure). Next, we denote $u_1^{\aleph}(t) = \left[u_{1,1}^{\aleph}(t)\ u_{1,2}^{\aleph}(t) \cdots u_{1,m}^{\aleph}(t)\right]^T$ and $\aleph(t) = \text{diag}\left\{\aleph_1(t)\ \ \aleph_2(t)\ \ \cdots\ \ \aleph_m(t)\right\}$. Hence, an uniform actuator fault model for primary controller is constructed as

$$u_1^{\aleph}(t) = (I_m - \aleph(t)) u_1(t) = (I_m - \aleph(t)) K_1 \hat{x}_1(t), \tag{7}$$

where K_1 represents the primary controller's state feedback control gain matrix and $0_m \leq \aleph(t) \leq \bar{\aleph} < I_m$. $\hat{x}_1(t)$ denotes the actual state input of $u_1^{\aleph}(t)$. Based on the above primary controller (7), we consider the secondary controller as

$$u_2(t) = u_1^{\aleph}(t) + K_2 \hat{x}_2(t), \tag{8}$$

where K_2 and $\hat{x}_2(t)$ denote the state feedback control gain and actual state input of secondary controller, respectively.

C. DESIGN OF AETM

In this study, we used the AETM, which is shown in FIGURE 1. Here, $t_k h$ be the current transmitted instant with h denotes the sampling period. In addition, the constraint for triggering instant $t_{k+1}h$ is expressed as

$$\begin{aligned} t_{k+1}h = t_k h + \min_{l \in N} \big\{ & lh | \mu_k^T(t_k h) \mathfrak{H} \mu_k(t_k h) \\ & - \chi(t) x_1^T(t_k h) \mathfrak{H} x_1(t_k h) > 0 \big\}, \end{aligned} \tag{9}$$

where $l = 1, 2, \cdots, \tilde{l}$ with $\tilde{l}$ denoting the maximum successive packet losses, $\chi(t)$ denotes threshold variable and it satisfies $0 < \chi(t) \leq 1$. $\mathfrak{H}$ being weighting positive definite matrix, and $\mu_k(t_k h) = x_1(t_k h + lh) - x_1(t_k h)$ in which $x_1(t_k h + lh)$ denotes the current sampling time and $x_1(t_k h)$ means latest transmitted data of the primary state.

The threshold variable $\chi(t)$ in (9) satisfies the following equality:

$$\dot{\chi}(t) = \frac{1}{\chi(t)}\left(\frac{1}{\chi(t)} - \vartheta\right)\mu_k^T(t_k h)\mathfrak{H}\mu_k(t_k h), \tag{10}$$

here, to adjust the convergence rate of $\chi(t)$, $\vartheta > 0$ is used. $0 < \chi(t) \leq 1$. Thus, the triggering constraint $\mu_k^T(t_k h)\mathfrak{H}\mu_k(t_k h) - \chi(t)x_1^T(t_k h)\mathfrak{H}x_1(t_k h) > 0$ can be dynamically modified according to the system states.

D. DoS ATTACK MODEL

In SNCCSs, the network is more vulnerable to malicious signals namely DoS attacks due to the communication channel's openness and the network environment's complexity. The frame work of SNCCSs with DoS attacks is given in FIGURE 1, where the duration and frequency of DoS attacks are restricted. When a network is subjected to DoS attacks, the actuator signals take the following form:

$$\begin{aligned}\hat{x}_1(t) &= \vartheta(t)x_{1e}(t),\\ \hat{x}_2(t) &= \vartheta(t)x_2(t),\end{aligned} \tag{11}$$

where $\vartheta(t)$ represents the DoS attack signals. In addition, $\vartheta(t) = 0$ or $\vartheta(t) = 1$ means DoS attacks occur or do not occur, respectively. $\vartheta(t) = 0$ means that the DoS signal is active when $t \in [b_n + \varkappa_n, b_{n+1})$; $\vartheta(t) = 1$ means that the DoS signal is inactive when $t \in [b_n, b_n + \varkappa_n)$. $n \in \mathbb{N}$ denotes the number of periods. b_{n+1} represents the end time of the n^{th} active period and the start time of the $(n+1)^{th}$ sleeping period; the length of the n^{th} sleeping period is denoted by $\varkappa_n$. It is obvious that the start and end times of the DoS sleeping period clearly satisfy the following conditions: $0 \leq b_0 < b_0 + \varkappa_0 < b_1 < b_1 + \varkappa_1 < b_2 < \cdots < b_n < b_n + \varkappa_n < b_{n+1} < \cdots$. $x_{1e}(t)$ is the standard signal sent over the network. For notation simplification, $\mathfrak{M}_{1,n} \triangleq [b_n, b_n + \varkappa_n)$ and $\mathfrak{M}_{2,n} \triangleq [b_n + \varkappa_n, b_{n+1})$ for all $n \in \mathbb{N}$.

E. EVENT-BASED CONTROLLER DESIGN

Due to the effect of the aperiodic DoS attacks, i.e., the transmitted data is interrupted in $\mathfrak{M}_{2,n}$, the ET condition (9) is not suitable, hence, this condition must be changed. Based on the above conditions and considering the impact of DoS attacks, the ET condition of the modified AETM can be expressed as follows:

$$t_{k,n}h = \left\{t_{k_c} \text{ satisfying (9)} | t_{k_c}h \in \mathfrak{M}_{1,n}\right\} \cup \{b_n\}, \tag{12}$$

where $n, k_c, c \in \mathbb{N}$ and k is the number of triggering instant in n-th DoS attack period such that $k \in \{1, 2, \cdots, k(n)\} \triangleq \mathcal{F}(n)$ and $k(n) = \sup\{k \in \mathbb{N} | t_{k,n}h \leq b_n + \varkappa_n\}$.

Remark 1: Based on the condition (12), we design resilient controllers for SNCCSs under DoS attacks. Moreover, the control law is constructed in the presence of DoS attacks as $u_1(t) = u_2(t) = 0$, when $t \in [b_n + \varkappa_n, b_{n+1})$. In addition, the control update policy is formulated while the absence of DoS attacks for $t \in [t_{k,n}h, t_{k+1,n}h) \cap [b_n, b_n + \varkappa_n)$.

For the sake of convenience, we assume $\mathcal{S}_{k,n} \triangleq [t_{k,n}h, t_{k+1,n}h)$, $t_{0,n}h \triangleq b_n$ for all $n \in \mathbb{N}$. Moreover, the interval $\mathcal{S}_{k,n}$ can be divided into

$$\mathcal{S}_{k,n} = \bigcup_{\upsilon=1}^{\varphi_{k,n}} \Upsilon_{k,n}^{\upsilon} \cup \Upsilon_{k,n}^{\varphi_{k,n}+1}, \tag{13}$$

where $n \in \mathbb{N}$, $k \in \mathcal{F}(n)$, $\varphi_{k,n} \triangleq \inf\{\upsilon \in \mathbb{N} | t_{k,n}h + \upsilon h \leq t_{k+1,n}h\}$, $\Upsilon_{k,n}^{\upsilon} = [t_{k,n}h + (\upsilon - 1)h, t_{k,n}h + \upsilon h)$, $\Upsilon_{k,n}^{\varphi_{k,n}+1} = [t_{k,n}h + \varphi_{k,n}h, t_{k+1,n}h)$ and $\upsilon \in \{1, \cdots, \varphi_{k,n}\}$.

Note that the following term holds:

$$\mathfrak{M}_{1,n} = \bigcup_{k=0}^{\mathcal{F}(n)} \left\{\mathcal{S}_{k,n} \cap \mathfrak{M}_{1,n}\right\} \subseteq \bigcup_{k=0}^{\mathcal{F}(n)} \mathcal{S}_{k,n}. \tag{14}$$

Based on (13) and (14), the interval $\mathfrak{M}_{1,n}$ is expressed as

$$\mathfrak{M}_{1,n} = \bigcup_{k=0}^{\mathcal{F}(n)} \bigcup_{\upsilon=1}^{\varphi_{k,n}+1} \left\{\Upsilon_{k,n}^{\upsilon} \cap \mathfrak{M}_{1,n}\right\}. \tag{15}$$

Accordingly, we define

$$d_{k,n}(t) = t - t_{k,n}h - (\bar{\iota} - 1)h, \quad t \in \Upsilon_{k,n}^{\bar{\iota}} \cap \mathfrak{M}_{1,n} \tag{16}$$

and

$$\mu_{k,n}(t) = x_1(t_{k,n}h) - x_1(t_{k,n}h + (\bar{\iota} - 1)h), \tag{17}$$

where $\bar{\iota} \in \{1, \cdots, \varphi_{k,n} + 1\}$.

From (16) and (17), it follows that $d_{k,n}(t) \in [0, h)$, and $t \in \mathcal{S}_{k,n} \cap \mathfrak{M}_{1,n}$. Hence, the sampled state $x_1(t_{k,n}h)$ is given as

$$x_{1e}(t) = x_1(t_{k,n}h) = x_1(t - d_{k,n}(t)) + \mu_{k,n}(t) \tag{18}$$

and the threshold variable $\chi(t)$ satisfies the constraint:

$$\dot{\chi}(t) = \tfrac{1}{\chi(t)}\left(\tfrac{1}{\chi(t)} - \vartheta\right)\mu_{k,n}^T(t)\mathfrak{H}\mu_{k,n}(t). \tag{19}$$

From (9) and (18), we get

$$\begin{aligned}\mu_{k,n}^T(t)\mathfrak{H}\mu_{k,n}(t) \leq\ & \chi(t)\left[x_1^T(t - d_{k,n}(t)) + \mu_{k,n}^T(t)\right]\\ & \times\mathfrak{H}\left[x_1(t - d_{k,n}(t)) + \mu_{k,n}(t)\right].\end{aligned} \tag{20}$$

Combining (1), (2), (6), (11), and (18), a new model for the SNCCS as

$$\begin{cases}\dot{x}_1(t) = A_1x_1(t) + B_1C_2x_2(t) + B_1D_2w(t),\\ E\dot{x}_2(t) = (A_2 + \mathcal{B}_1)x_2(t) + A_3x_2(t - \tau(t))\\ -B_2\Xi(u_2(t)) + \mathbf{B}_1\left[x_1(t - d_{k,n}(t)) + \mu_{k,n}(t)\right]\\ +B_3w(t), \quad t \in \mathfrak{M}_{1,n}\\ y_1(t) = C_1x_1(t) + D_1w(t),\end{cases} \tag{21}$$

$$\begin{cases}\dot{x}_1(t) = A_1x_1(t) + B_1C_2x_2(t) + B_1D_2w(t),\\ E\dot{x}_2(t) = A_2\bar{x}_2(t) + A_3x_2(t - \tau(t)) + B_3w(t),\\ y_1(t) = C_1x_1(t) + D_1w(t), \quad t \in \mathfrak{M}_{2,n}\end{cases} \tag{22}$$

where $\mathcal{B}_1 = B_2K_2$ and $\mathbf{B}_1 = B_2(I - \aleph(t))K_1$. For simplicity of notation, we define $\varepsilon(t) = 1$ for $t \in [-h, 0] \cup (\cup\, \mathfrak{M}_{1,n})$

and if $\varepsilon(t) = 2$ for $t \in \mathfrak{M}_{2,n}$. For $\varepsilon(t) = q \in \{1, 2\}$, by letting that

$$t_{q,n} = \begin{cases} b_n, & q = 1 \\ b_n + \varkappa_n, & q = 2 \end{cases} \tag{23}$$

we get $\mathfrak{M}_{q,n} = [t_{q,n}, t_{3-q,n+q-1})$. According to (21) and (22), the switched system is obtained as

$$\begin{cases} \dot{x}_1(t) = A_1 x_1(t) + B_1 C_2 x_2(t) + B_1 D_2 w(t), \\ E\dot{x}_2(t) = (A_2 + \mathcal{B}_q) x_2(t) + A_3 x_2(t - \tau(t)) \\ -\bar{\mathcal{B}}_q \Xi(u_2(t)) + \mathbf{B}_q \Big[x_1(t - d_{k,n}(t)) + \mu_{k,n}(t) \Big] \\ +B_3 w(t), \quad t \in [t_{q,n}, t_{3-q,n+q-1}), \ q = 1, 2, \\ y_1(t) = C_1 x_1(t) + D_1 w(t), \end{cases} \tag{24}$$

where $\bar{\mathcal{B}}_1 = B_2$ and $\mathcal{B}_2 = \bar{\mathcal{B}}_2 = \mathbf{B}_2 = 0$.

To achieve the main results, the definitions and assumptions listed below are used.

Definition 2: The SNCCS (24) with $w(t) = 0$

(1) The pair (E, A_2) is said to be regular and impulse free, respectively, if $\det(sE - A_2)$ is not identically zero and $\deg(\det(sE - A_2)) = \text{rank}(E)$.
(2) If the pair (E, A_2) is regular and impulse free, the unforced singular system is also regular and impulse free.
(3) The SNCCS (24) with $w(t) = 0$ is said to be exponentially stable, if positive constants $\bar{u}$ and $\bar{v}$ exist such that $\|x_2(t)\|^2 \leq \bar{u} e^{-\bar{v}t} \|\phi(t)\|^2$.
(4) If the SNCCS (24) is regular, impulse-free, and exponentially stable, it is said to be exponentially admissible.

Definition 3: For the given real matrices $\Lambda_1 = \Lambda_1^T \leq 0$, Λ_2, $\Lambda_3 = \Lambda_3^T > 0$, and $\Lambda_4 = \Lambda_4^T \geq 0$ satisfying $(\|\Lambda_1\| + \|\Lambda_2\|)\Lambda_4 = 0$, the SNCCS (24) is said to be extended dissipative if the following inequality holds for any $t_f \geq 0$ and $w(t) \in L_2[0, \infty)$:

$$\int_0^{t_f} \mathbf{J}(t) dt \geq \sup_{0 \leq t \leq t_f} y_1^T(t) \Lambda_4 y_1(t),$$

where $\mathbf{J}(t) = y_1^T(t)\Lambda_1 y_1(t) + 2y_1^T(t)\Lambda_2 w(t) + w^T(t)\Lambda_3 w(t)$.

Intuitively, the choice of intervals $\mathfrak{M}_{1,n}$ and $\mathfrak{M}_{2,n}$ must not be completely arbitrary, since both the duration and frequency of DoS must be limited in order to achieve admissibility. In light of this, the following assumptions are considered.

Assumption 4: **(DoS Duration)** Let $\Upsilon(0, t) = \cup_{n \in \mathbb{N}} \mathfrak{M}_{2,n} \bigcap [0, t]$ denote the total interval of DoS attacks over $[0, t]$. There exists $\iota \in \mathbb{R}_{\geq 0}$ and $\omega_G \in \mathbb{R}_{>1}$ such that $|\Upsilon(0, t)| \leq \iota + \frac{t}{\omega_G}$.

Assumption 5: **(DoS Frequency)** Let $n(t)$ represent the number of DoS off/on transitions in the range $[0, t)$, i.e., $n(t) = card\{n \in \mathbb{N} | b_n + \varkappa_n < t\}$, where *card* denotes the number of elements in the set. $\exists\ \breve{\iota} \in \mathbb{R}_{\geq 0}$, $\omega_D \in \mathbb{R}_{>0}$ such that $n(0, t) \leq \breve{\iota} + \frac{t}{\omega_D}$.

Remark 6: This paper does not discuss the rationality of Assumptions 4 and 5, which have been extensively discussed in [9] and [12].

Remark 7: From the proposed AETM (9) in this paper, the threshold variable $\chi(t)$ has a significant impact on the number of packets transmitted over the network in a given period. $\chi(t)$ is an optimal result regulated by the adaptive law (10) on-line, while the predefined threshold scalar σ in [18], by which it can not be accommodated with varying external disturbance.

III. MAIN RESULTS

A. STABILITY ANALYSIS

In this subsection, according to the Wirtinger-based integral inequality approach, we obtain a set of sufficient conditions for the exponential admissibility of SNCCS (24) with known actuator fault matrix $\bar{\aleph}$ and aperiodic DoS attacks.

Theorem 8: For the given scalars δ_q, $\daleth_q$, $h_\tau = \max\{h, \tau_2\}$, trigger parameter ϑ, DoS parameters $\omega_G \in \mathbb{R}_{>0}$ and $\omega_D \in \mathbb{R}_{>1}$ satisfying

$$\mathcal{I} := 2\delta_1 - \frac{2(\delta_1 + \delta_2)h_\tau + \ln(\daleth_1 \daleth_2)}{\omega_G} - \frac{2(\delta_1 + \delta_2)}{\omega_D} > 0, \tag{25}$$

matrices Λ_1, Λ_2, Λ_3, Λ_4 satisfying Definition 3, actuator fault matrix $\bar{\aleph}$, primary gain K_1 and secondary gain K_2 are known, the system (24) is exponentially admissible and satisfies extended dissipative, if there exists symmetric matrices $O_{kq} > 0$, $\mathfrak{H} > 0$, $O \in \{P, Q, R, Z\}$, such that for $k, q = 1, 2$, the following LMIs hold:

$$\Omega^q < 0, \tag{26}$$
$$P_{k1} \leq \daleth_2 P_{k2}, \tag{27}$$
$$P_{k2} \leq \daleth_1 e^{2(\delta_1 + \delta_2)h_\tau} P_{k1}, \tag{28}$$
$$W_{kq} \leq \daleth_{3-q} W_{k(3-q)}, \quad W \in \{Q, R, Z\} \tag{29}$$
$$P_{1q} - C_1^T \Lambda_4 C_1 \geq 0, \tag{30}$$
$$E^T P_{2q} = P_{2q}^T E \geq 0, \tag{31}$$

where

$$\Omega^1 = \begin{bmatrix} \Omega^1_{13\times 13} & \Omega^1_1 & \Omega^1_2 & \Omega^1_3 & \Omega^1_4 \\ * & -Z_{11}^{-1} & 0 & 0 & 0 \\ * & * & -Z_{21}^{-1} & 0 & 0 \\ * & * & * & -I & 0 \\ * & * & * & * & -I \end{bmatrix},$$

$$\Omega^2 = \begin{bmatrix} \Omega^2_{11\times 11} & \Omega^2_1 & \Omega^2_2 & \Omega^2_4 \\ * & -Z_{12}^{-1} & 0 & 0 \\ * & * & -Z_{22}^{-1} & 0 \\ * & * & * & -I \end{bmatrix},$$

$$\begin{aligned} \Omega^q_{1,1} &= P_{1q}A_1 + A_1^T P_{1q} + Q_{1q} - 4e^{2(-1)^q \delta_q h} Z_{1q} \\ &\quad - 2(-1)^q \delta_q P_{1q}, \\ \Omega^q_{1,2} &= -2e^{2(-1)^q \delta_q h} Z_{1q}, \\ \Omega^q_{1,4} &= 6e^{2(-1)^q \delta_q h} Z_{1q}, \\ \Omega^q_{1,6} &= P_{1q} B_1 C_2, \\ \Omega^1_{1,13} &= P_{11} B_1 C_2 - C_1^T \Lambda_2, \\ \Omega^2_{1,11} &= P_{12} B_1 C_2 - C_1^T \Lambda_2, \\ \Omega^1_{2,2} &= -8e^{-2\delta_1 h} Z_{11} + \vartheta \mathfrak{H}, \\ \Omega^2_{2,2} &= -8e^{2\delta_2 h} Z_{12}, \end{aligned}$$

$$
\begin{aligned}
\Omega^q_{2,3} &= -2e^{2(-1)^q\delta_q h}Z_{1q},\\
\Omega^q_{2,4} &= 6e^{2(-1)^q\delta_q h}Z_{1q},\\
\Omega^q_{2,5} &= 6e^{2(-1)^q\delta_q h}Z_{1q},\\
\Omega^1_{2,6} &= \hat{\mathbf{B}}_1^T P_{21}^T,\\
\Omega^1_{2,11} &= \vartheta\mathfrak{H},\\
\Omega^q_{3,3} &= -e^{2(-1)^q\delta_q h}(Q_{1q}+4Z_{1q}),\\
\Omega^q_{3,5} &= 6e^{2(-1)^q\delta_q h}Z_{1q},\\
\Omega^q_{4,4} &= -12e^{2(-1)^q\delta_q h}Z_{1q},\\
\Omega^q_{5,5} &= -12e^{2(-1)^q\delta_q h}Z_{1q},\\
\Omega^1_{6,6} &= P_{21}A_2 + A_2^T P_{21} + 2P_{21}\mathcal{B}_1 + Q_{21} + R_{1q} + \tau_2 R_{21}\\
&\quad + 2\delta_1 E^T P_{21} - 4e^{-2\delta_1\tau_2}E^T Z_{21}E,\\
\Omega^2_{6,6} &= P_{22}A_2 + A_2^T P_{22} + Q_{22} + R_{12} + \tau_2 R_{22} - 2\delta_2 E^T P_{22}\\
&\quad - 4e^{2\delta_2\tau_2}E^T Z_{22}E,\\
\Omega^q_{6,7} &= P_{2q}A_3 - 2e^{2(-1)^q\delta_q\tau_2}E^T Z_{2q}E,\\
\Omega^q_{6,9} &= 6e^{2(-1)^q\delta_q\tau_2}E^T Z_{2q}E,\\
\Omega^1_{6,11} &= P_{21}\hat{\mathbf{B}}_1,\\
\Omega^1_{6,12} &= -P_{21}\bar{\mathcal{B}}_1,\\
\Omega^1_{6,13} &= P_{21}B_3,\\
\Omega^2_{6,11} &= P_{22}B_3,\\
\Omega^q_{7,7} &= -(1-\nu)e^{2(-1)^q\delta_q\tau_2}R_{1q} - 8e^{2(-1)^q\delta_q\tau_2}E^T Z_{2q}E,\\
\Omega^q_{7,8} &= -2e^{2(-1)^q\delta_q\tau_2}E^T Z_{2q}E,\\
\Omega^q_{7,9} &= 6e^{2(-1)^q\delta_q\tau_2}E^T Z_{2q}E,\\
\Omega^q_{7,10} &= 6e^{2(-1)^q\delta_q\tau_2}E^T Z_{2q}E,\\
\Omega^q_{8,8} &= -e^{2(-1)^q\delta_q\tau_2}(Q_{2q}+4E^T Z_{2q}E),\\
\Omega^q_{8,10} &= 6e^{2(-1)^q\delta_q\tau_2}E^T Z_{2q}E,\\
\Omega^q_{9,9} &= -12e^{2(-1)^q\delta_q\tau_2}E^T Z_{2q}E - \frac{1}{\tau_2}R_{2q},\\
\Omega^q_{10,10} &= -12e^{2(-1)^q\delta_q\tau_2}E^T Z_{2q}E - \frac{1}{\tau_2}R_{2q},\\
\Omega^1_{11,11} &= -\mathfrak{H},\\
\Omega^1_{12,12} &= -I,\\
\Omega^1_{13,13} &= -2D_1^T\Lambda_2 - \Lambda_3,\\
\Omega^2_{11,11} &= -2D_1^T\Lambda_2 - \Lambda_3,\\
\Omega^1_1 &= \begin{bmatrix}A_1 & 0_{1\times4} & B_1C_2 & 0_{1\times6} & B_1D_2\end{bmatrix}^T,\\
\Omega^1_2 &= \begin{bmatrix}0 & \hat{\mathbf{B}}_1 & 0_{1\times3} & (A_2+\mathcal{B}_1) & A_3 & 0_{1\times3} & \hat{\mathbf{B}}_1 & -\bar{\mathcal{B}}_1 & B_3\end{bmatrix},\\
\Omega^1_3 &= \begin{bmatrix}0 & \sqrt{\epsilon}\mathfrak{I}K_1 & 0_{1\times3} & \sqrt{\epsilon}K_2 & 0_{1\times4} & \sqrt{\epsilon}\mathfrak{I}K_1 & 0 & 0\end{bmatrix}^T,\\
\Omega^1_4 &= \begin{bmatrix}\hat{\Lambda}_1C_1 & 0_{1\times11} & \hat{\Lambda}_1D_1\end{bmatrix}^T,\\
\Omega^2_1 &= \begin{bmatrix}A_1 & 0_{1\times4} & B_1C_2 & 0_{1\times4} & B_1D_2\end{bmatrix}^T,\\
\Omega^2_2 &= \begin{bmatrix}0_{1\times5} & A_2 & A_3 & 0_{1\times3} & B_3\end{bmatrix}^T,\\
\Omega^2_4 &= \begin{bmatrix}\hat{\Lambda}_1C_1 & 0_{1\times9} & \hat{\Lambda}_1D_1\end{bmatrix}^T,\\
\mathfrak{I} &= (I-\bar{\aleph}) \text{ and } \hat{\mathbf{B}}_1 = B_2(I-\bar{\aleph})K_1.
\end{aligned}
$$

Proof: To obtain that the system (24) with $w(t) = 0$ is admissible, we first prove that the system (24) is exponentially stable. For this purpose, we choose the LKF candidate as

$$V_q(t) = V_{1q}(t) + V_{2q}(t) + V_{3q}(t) + V_{4q}(t), \tag{32}$$

where

$$
\begin{aligned}
V_{1q}(t) &= x_1^T(t)P_{1q}x_1(t) + x_2^T(t)E^T P_{2q}x_2(t),\\
V_{2q}(t) &= \int_{t-h}^{t} f(\bullet)x_1^T(s)Q_{1q}x_1(s)ds\\
&\quad + \int_{t-\tau_2}^{t} f(\bullet)x_2^T(s)Q_{2q}x_2(s)ds,\\
V_{3q}(t) &= \int_{t-\tau(t)}^{t} f(\bullet)x_2^T(s)R_{1q}x_2(s)ds\\
&\quad + \int_{-\tau_2}^{0}\int_{t+\theta}^{t} f(\bullet)x_2^T(s)R_{2q}x_2(s)dsd\theta,\\
V_{4q}(t) &= h\int_{-h}^{0}\int_{t+\theta}^{t} f(\bullet)\dot{x}_1^T(s)Z_{1q}\dot{x}_1(s)dsd\theta\\
&\quad + \tau_2\int_{-\tau_2}^{0}\int_{t+\theta}^{t} f(\bullet)\dot{x}_2^T(s)E^T Z_{2q}E\dot{x}_2(s)dsd\theta
\end{aligned}
$$

with $f(\bullet) = e^{(-1)^q 2\delta_q(t-s)}$.

If we fix $q = 1$, by taking the derivative of $V_1(t)$ with respect to time t, we obtain that

$$
\begin{aligned}
\dot{V}_{11}(t) &= -2\delta_1 V_{11}(t) + 2\delta_1 x_1^T(t)P_{11}x_1(t) + 2x_1^T(t)P_{11}\dot{x}_1(t)\\
&\quad + 2\delta_1 x_2^T(t)E^T P_{21}x_2(t)\\
&\quad + 2x_2^T(t)P_{21}E\dot{x}_2(t), \qquad (33)\\
\dot{V}_{21}(t) &=\\
&\quad - 2\delta_1 V_{21}(t) + x_1^T(t)Q_{11}x_1(t) + x_2^T(t)Q_{21}x_2(t)\\
&\quad - e^{-2\delta_1 h}x_1^T(t-h)Q_{11}x_1(t-h)\\
&\quad - e^{-2\delta_1\tau_2}x_2^T(t-\tau_2)Q_{21}x_2(t-\tau_2), \qquad (34)\\
\dot{V}_{31}(t) &\le\\
&\quad - 2\delta_1 V_{31}(t)\\
&\quad + x_2^T(t)R_{11}x_2(t)\\
&\quad + \tau_2 x_2^T(t)R_{21}x_2(t)\\
&\quad - (1-\nu)e^{-2\delta_1\tau_2}x_2^T(t-\tau(t))R_{11}x_2(t-\tau(t)) \qquad (35)\\
&\quad - \int_{t-\tau_2}^{t} e^{-2\delta_1\tau_2}x_2^T(s)R_{21}x_2(s)ds,\\
\dot{V}_{41}(t) &\le\\
&\quad - 2\delta_1 V_{41}(t)\\
&\quad + h^2\dot{x}_1^T(t)Z_{11}\dot{x}_1(t)\\
&\quad + \tau_2^2\dot{x}_2^T(t)E^T Z_{21}E\dot{x}_2(t)\\
&\quad - h\int_{t-h}^{t} e^{-2\delta_1 h}\dot{x}_1^T(s)Z_{11}\dot{x}_1(s)ds\\
&\quad - \tau_2\int_{t-\tau_2}^{t} e^{-2\delta_1\tau_2}\dot{x}_2^T(s)E^T Z_{21}E\dot{x}_2(s)ds. \qquad (36)
\end{aligned}
$$

By applying the time delay intervals to the integral terms in $\dot{V}_{41}(t)$, the following can be obtained:

$$\begin{aligned}-\int_{t-h}^{t}\dot{x}_1^T(s)Z_{11}\dot{x}_1(s)ds &= -\int_{t-h}^{t-d_{k,n}(t)}\dot{x}_1^T(s)Z_{11}\dot{x}_1(s)ds \\ &\quad -\int_{t-d_{k,n}(t)}^{t}\dot{x}_1^T(s)Z_{11}\dot{x}_1(s)ds,\end{aligned} \tag{37}$$

$$\begin{aligned}-\int_{t-\tau_2}^{t}\dot{x}_2^T(s)E^TZ_{21}E\dot{x}_2(s)ds &= -\int_{t-\tau_2}^{t-\tau(t)}\dot{x}_2^T(s)E^TZ_{21}E\dot{x}_2(s)ds \\ &\quad -\int_{t-\tau(t)}^{t}\dot{x}_2^T(s)E^TZ_{21}E\dot{x}_2(s)ds.\end{aligned} \tag{38}$$

By using Wirtinger-based integral inequality to the above inequalities, we obtain that

$$-\int_{t-h}^{t-d_{k,n}(t)}\dot{x}_1^T(s)Z_{11}\dot{x}_1(s)ds \le -\frac{1}{h}\zeta_1^T\Lambda^T\mathfrak{Z}_1\Lambda\zeta_1, \tag{39}$$

$$-\int_{t-d_{k,n}(t)}^{t}\dot{x}_1^T(s)Z_{11}\dot{x}_1(s)ds \le -\frac{1}{h}\zeta_2^T\Lambda^T\mathfrak{Z}_1\Lambda\zeta_2, \tag{40}$$

$$-\int_{t-\tau_2}^{t-\tau(t)}\dot{x}_2^T(s)E^TZ_{21}E\dot{x}_2(s)ds \le -\frac{1}{\tau_2}\zeta_3^T\Lambda^T\mathfrak{Z}_2\Lambda\zeta_3, \tag{41}$$

$$-\int_{t-\tau(t)}^{t}\dot{x}_2^T(s)E^TZ_{21}E\dot{x}_2(s)ds \le -\frac{1}{\tau_2}\zeta_4^T\Lambda^T\mathfrak{Z}_2\Lambda\zeta_4, \tag{42}$$

where

$$\zeta_1 = \begin{bmatrix} x_1^T(t-d_{k,n}(t))\ x_1(t-h) & \frac{1}{h-d_{k,n}(t)} \\ & \times\int_{t-h}^{t-d_{k,n}(t)}x_1^T(s)ds \end{bmatrix}^T$$

$$\zeta_2 = \left[x_1(t)\ x_1^T(t-d_{k,n}(t))\ \tfrac{1}{d_{k,n}(t)}\int_{t-d_{k,n}(t)}^{t}x_1^T(s)ds\right]^T,$$

$$\zeta_3 = \left[x_2^T(t-\tau(t))\ x_2(t-\tau_2)\ \tfrac{1}{\tau_2-\tau(t)}\int_{t-\tau_2}^{t-\tau(t)}x_2^T(s)ds\right]^T,$$

$$\zeta_4 = \left[x_2(t)\ x_2^T(t-\tau(t))\ \tfrac{1}{\tau(t)}\int_{t-\tau(t)}^{t}x_2^T(s)ds\right]^T,$$

$$\mathfrak{Z}_1 = \begin{bmatrix} Z_{11} & 0 \\ 0 & 3Z_{11}\end{bmatrix},$$

$$\mathfrak{Z}_2 = \begin{bmatrix} E^TZ_{21}E & 0 \\ 0 & 3E^TZ_{21}E\end{bmatrix},$$

and $\Lambda = \begin{bmatrix} I_n & -I_n & 0 \\ I_n & I_n & -2I_n.\end{bmatrix}$

By using Jensen's inequality to the integral term in $\dot{V}_{31}(t)$, the following relationship holds.

$$\begin{aligned}-\int_{t-\tau_2}^{t}x_2^T(s)R_{21}x_2(s)ds \le \frac{-1}{\tau_2}&\begin{bmatrix}\int_{t-\tau_2}^{t-\tau(t)}x_2(s)ds \\ \int_{t-\tau(t)}^{t}x_2(s)ds\end{bmatrix}^T \\ &\times\begin{bmatrix}R_{21} & 0 \\ * & R_{21}\end{bmatrix}\begin{bmatrix}\int_{t-\tau_2}^{t-\tau(t)}x_2(s)ds \\ \int_{t-\tau(t)}^{t}x_2(s)ds\end{bmatrix}.\end{aligned} \tag{43}$$

Next, by combining (5), (20), (24), (33)-(43) and using Schur complement lemma, it yields that

$$\dot{V}_1(t) \le -2\delta_1V_1(t) + \xi_1^T(t)\Theta^1\xi_1(t), \tag{44}$$

where

$$\Theta^1 = \begin{bmatrix}\bar{\Omega}_{12\times12}^1 & \bar{\Omega}_1^1 & \bar{\Omega}_2^1 & \bar{\Omega}_3^1 \\ * & -Z_{11}^{-1} & 0 & 0 \\ * & * & -Z_{21}^{-1} & 0 \\ * & * & * & -I\end{bmatrix},$$

$$\bar{\Omega}_{12\times12}^1 = \Omega_{12\times12}^1,\ \bar{\Omega}_1^1 = \begin{bmatrix}A_1\ 0_{1\times4}\ B_1C_2\ 0_{1\times6}\end{bmatrix}^T,$$

$$\bar{\Omega}_2^1 = \begin{bmatrix}0\ \hat{\mathbf{B}}_1\ 0_{1\times3}\ (A_2+\mathcal{B}_1)\ A_3\ 0_{1\times3}\ \hat{\mathbf{B}}_1\ -\bar{\mathcal{B}}_1\end{bmatrix}^T,$$

$$\bar{\Omega}_3^1 = \begin{bmatrix}0\ \sqrt{\epsilon}\mathfrak{J}K_1\ 0_{1\times3}\ \sqrt{\epsilon}K_2\ 0_{1\times4}\ \sqrt{\epsilon}\mathfrak{J}K_1\ 0\end{bmatrix}^T,$$

$$\xi_1(t) = \begin{bmatrix}\eta(t)\ \mu_{k,n}^T(t)\ \Xi^T(u_2(t))\ I\ I\ I\end{bmatrix}$$

with

$$\begin{aligned}\eta(t) = \big[&x_1^T(t)\ x_1^T(t-d_{k,n}(t))\ x_1^T(t-h) \\ &\tfrac{1}{d_{k,n}(t)}\int_{t-d_{k,n}(t)}^{t}x_1^T(s)ds\ \tfrac{1}{h-d_{k,n}(t)}\int_{t-h}^{t-d_{k,n}(t)}x_1^T(s)ds \\ &x_2^T(t)\ x_2^T(t-\tau(t))\ x_2(t-\tau_2) \\ &\tfrac{1}{\tau(t)}\int_{t-\tau(t)}^{t}x_2^T(s)ds\ \tfrac{1}{\tau_2-\tau(t)}\int_{t-\tau_2}^{t-\tau(t)}x_2^T(s)ds\big].\end{aligned}$$

Since $\Theta^1 < 0$ is ensured by (26), it yields that $\dot{V}_1(t) \le -2\delta_1V_1(t)$.

When $q = 2$, by taking the derivative of $V_2(t)$ and by using the similar approach for case $q = 1$, we have

$$\dot{V}_2(t) \le 2\delta_2V_2(t) + \xi_2^T(t)\Theta^2\xi_2(t), \tag{45}$$

where $\Theta^2 = \begin{bmatrix}\bar{\Omega}_{10\times10}^2 & \bar{\Omega}_1^2 & \bar{\Omega}_2^2 \\ * & -Z_{12}^{-1} & 0 \\ * & * & -Z_{22}^{-1}\end{bmatrix}$, $\bar{\Omega}_{10\times10}^2 = \Omega_{10\times10}^2$, $\bar{\Omega}_1^2 = \begin{bmatrix}A_1\ 0_{1\times4}\ B_1C_2\ 0_{1\times4}\end{bmatrix}^T$, $\bar{\Omega}_2^2 = \begin{bmatrix}0_{1\times5}\ A_2\ A_3\ 0_{1\times3}\end{bmatrix}^T$, and $\xi_2(t) = \begin{bmatrix}\eta(t)\ I\ I\end{bmatrix}$. According to the $\Theta^2 < 0$ which is ensured by (26), it yields $\dot{V}_2(t) \le 2\delta_2V_2(t)$.

Inspired by [28], one has from (44)-(45) that

$$V(t) = \begin{cases} e^{-2\delta_1(t-b_n)})V_1(b_n), & t\in[b_n, b_n+\varkappa_n) \\ e^{2\delta_2(t-b_n-\varkappa_n)})V_2(b_n+\varkappa_n), & t\in[b_n+\varkappa_n, b_{n+1}).\end{cases} \tag{46}$$

From (27)-(29), we get

$$\begin{cases} \daleth_2V_2(b_n^-) - V_1(b_n) \ge 0 \\ e^{2(\delta_1+\delta_2)h}\daleth_1V_1(b_n^- + \varkappa_n^-)\ - V_2(b_n+\varkappa_n) \ge 0.\end{cases} \tag{47}$$

For all $t \geq 0$, then it can be divided as $t \in [b_n, b_n + \varkappa_n)$ and $t \in [b_n + \varkappa_n, b_{n+1})$. In the first case $t \in [b_n, b_n + \varkappa_n)$, it follows from (46) and (47) that

$$\begin{aligned} V_1(t) &\leq \urcorner_2 e^{-2\delta_1(t-b_n)} V_2(b_n^-) \\ &\leq \urcorner_2 e^{-2\delta_1(t-(b_{n-1}+\varkappa_{n-1}))+2(\delta_1+\delta_2)(b_n-(b_{n-1}+\varkappa_{n-1}))} \\ &\quad \times V_2(b_{n-1}+\varkappa_{n-1}) \\ &\leq \cdots \\ &\leq e^{-2\delta_1 t+\varrho_1(t,0)} V_1(0). \end{aligned} \tag{48}$$

Similarly, when $t \in [b_n + \varkappa_n, \varkappa_{n+1})$, by using the similar procedure as presented in the above case, we get

$$V_2(t) \leq \frac{e^{-2\delta_1 t+\varrho_1(t,0)}}{\urcorner_2} V_1(0). \tag{49}$$

From Assumptions 4, 5, the use of (48) yields that

$$V(t) \leq e^{\mathcal{F}} e^{-\mathcal{I}t} V_1(0), \tag{50}$$

where $\mathcal{F} = (2(\delta_1+\delta_2)h_\tau + \ln(\urcorner_1 \urcorner_2))\iota + 2(\delta_1+\delta_2)\check{\iota}$. Similarly, using (49), Assumptions 4 and 5 yield that

$$V(t) \leq \frac{e^{\mathcal{F}} e^{-\mathcal{I}t}}{\urcorner_2} V_1(0). \tag{51}$$

From the definition of $V(t)$, we get that

$$\mathfrak{F}_1 \|\phi\|_h^2 \geq V_1(0), \quad \mathfrak{F}_2 \|x(t)\|^2 \leq V(t), \tag{52}$$

where $\mathfrak{F}_1 = \mathfrak{F}_3 + \max\left\{\lambda_{\max} P_{1q} + h\lambda_{\max} Q_{1q} + \frac{h^2}{2}\lambda_{\max} Z_{1q}\right\}$ with $\mathfrak{F}_3 = \max\left\{\lambda_{\max} P_{1q}\right\}$ and $\mathfrak{F}_2 = \min\left\{\lambda_{\min} P_{1q}\right\}$. Hence, from (50)-(52), we have that

$$\|x_1(t)\|^2 \leq \frac{\mathfrak{F}_2}{\mathfrak{F}_1} e^{-\mathcal{I}t} \|\phi\|_h^2. \tag{53}$$

According to Definition 2, it is clear that the system (24) is exponentially stable with decay rate $\mathcal{I}$. By using the similar method, we can complete the proof for the secondary plant. Hence, it is omitted here.

Next, we shall prove that the system (24) is impulse-free and regularity. In doing so, we let the singular matrix $\hat{E}$ and state vector $x_2(t)$ have the following forms:

$$x_2(t) = \begin{bmatrix} x_{21}(t) \\ x_{22}(t) \end{bmatrix} \quad \text{and} \quad \hat{E} = \begin{bmatrix} I_r & 0_{r\times(n-r)} \\ 0_{(n-r)\times r} & 0_{(n-r)} \end{bmatrix},$$

where $x_{21}(t) \in \mathbb{R}^r$ and $x_{22}(t) \in \mathbb{R}^{(n-r)}$. Then, it follows from (44) and (45) that

$$\Omega_{6,6}^q = Q_{2q} + 2P_{2q}\hat{A}_2. \tag{54}$$

Next, we define

$$P_{2q} = \begin{bmatrix} P_{21q} & P_{22q} \\ P_{23q} & P_{24q} \end{bmatrix}, \; A_2 = \begin{bmatrix} A_{21} & A_{22} \\ A_{23} & A_{24} \end{bmatrix}, \; Q_{2q} = \begin{bmatrix} Q_{1q} & Q_{2q} \\ Q_{3q} & Q_{4q} \end{bmatrix}.$$

By substituting P_{2q}, $\hat{A}_2$, and Q_{2q} into (54), it yields that

$$(P_{24q}A_{24} + A_{24}^T P_{24q}^T) + Q_{4q} < 0.$$

Then, it obvious that $\det(s\hat{E} - \hat{A}_2) = \det(sE - A_2)$ which tends to $\det(sE - A_2)$ is not identically zero and $\det(sE - A_2) = r = \text{rank}(E)$. Hence, the system (24) is regular and impulse free. Based on the Definition 2, the system (24) is therefore exponentially admissible.

From Definition 3 and system (24) with disturbances, we get

$$\begin{cases} \dot{V}_1(t) + 2\delta_1 V_1(t) - \mathbf{J}(t) \leq \bar{\xi}_1^T(t)\bar{\Omega}^1\bar{\xi}_1(t), \\ \dot{V}_2(t) - 2\delta_2 V_2(t) - \mathbf{J}(t) \leq \bar{\xi}_2^T(t)\bar{\Omega}^2\bar{\xi}_2(t), \end{cases} \tag{55}$$

where $\bar{\xi}_1(t) = \left[\eta(t)\ \mu_{k,n}^T(t)\ \Xi^T(u_2(t))\ w^T(t)\ I\ I\ I\ I\right]$, $\bar{\xi}_2(t) = \left[\eta(t)\ w^T(t)\ I\ I\ I\right]$. Next, by integrating both sides of (55) from 0 to $t \geq 0$, we get

$$\int_0^t \mathbf{J}(s)ds \geq V(t) - V(0) \geq x_1^T(t)P_{1q}x_1(t) \tag{56}$$

Based on the extended dissipative definition (Definition 3), the following condition holds for any matrices Λ_1, Λ_2, Λ_3, Λ_4 satisfying:

$$\int_0^{t_f} \mathbf{J}(s)ds \geq \sup_{0\leq t\leq t_f} y_1^T(t)\Lambda_4 y_1(t), \tag{57}$$

where t_f is any nonnegative scalar. Due to the extended dissipative condition, Λ_4 is divided into two cases, namely $\Lambda_4 = 0$ and $\Lambda_4 > 0$. The first case involves the strict $(\mathcal{Q}, \mathcal{S}, \mathcal{R})$-dissipative condition as well as passivity and H_∞ performance. When $\Lambda_4 > 0$, the $L_2 - L_\infty$ performance criterion is satisfied.

Firstly, by considering that $\Lambda_4 = 0$, we have

$$\int_0^{t_f} \mathbf{J}(s)ds \geq 0,$$

which implies the extended dissipative definition with $\Lambda_4 = 0$.

In the second case with $\Lambda_4 > 0$, as given in Definition 3, we have the following matrices $\Lambda_1 = 0$, $\Lambda_2 = 0$, $\Lambda_3 > 0$ with $\|\Lambda_1\| + \|\Lambda_2\| = 0$ and $\|D_1\| = 0$. For any $t \in [0, t_f]$ and (56), we get $\int_0^{t_f} \mathbf{J}(s)ds \geq \int_0^{t_f} \mathbf{J}(s)ds \geq x_1^T(t)P_{1q}x_1(t)$. Hence, from (30), we have

$$\begin{aligned} y_1^T(t)\Lambda_4 y_1(t) &= x_1^T(t)C_1^T\Lambda_4 C_1 x_1(t) \leq x_1^T(t)P_{1q}x_1(t) \\ &\leq \int_0^{t_f} \mathbf{J}(s)ds. \end{aligned} \tag{58}$$

Therefore, the above results discuss two cases of Λ_4. It is easy to conclude that system (24) is extended dissipative for any $w(t) \neq 0$ based on Definition 3, which ends the proof.

B. ADAPTIVE EVENT-TRIGGERED EXTENDED DISSIPATIVE CONTROL DESIGN

By using the above theorem, we derive the primary and secondary controller gain matrices and the associated sufficient conditions that guarantee the system (24) being exponentially admissible as stated in the following theorem.

Theorem 9: For the given scalars δ_q, $\urcorner_q$, $h_\tau = \max\{h, \tau_2\}$, $\digamma_{kq}$, ε_{kq}, φ_{kq}, ς_{kq}, trigger parameter ϑ, DoS parameters $\omega_G \in \mathbb{R}_{>0}$ and $\omega_D \in \mathbb{R}_{>1}$ satisfying (25), matrices Λ_1, Λ_2, Λ_3, Λ_4 satisfying Definition 3, known fault matrix $\aleph$, the primary and secondary gains are computed as $Y_1 = K_1 X_{11}$ and $Y_2 =$

K_2X_{21}, respectively. Then, the system (24) is exponentially admissible and satisfies the extended dissipative condition, if there exists symmetric matrices $\tilde{O}_{kq} > 0$, $\tilde{\mathfrak{H}} > 0$, $\tilde{O} \in \{\tilde{P}, \tilde{Q}, \tilde{R}, \tilde{Z}\}$, such that for $k, q = 1, 2$, the following LMIs hold:

$$\Phi^q < 0, \tag{59}$$

$$\begin{bmatrix} -\urcorner_2 X_{k2} & X_{k2} \\ * & -X_{k1} \end{bmatrix} \leq 0, \tag{60}$$

$$\begin{bmatrix} -\urcorner_1 e^{2(\delta_1+\delta_2)h_\tau} X_{k1} & X_{k1} \\ * & -X_{k2} \end{bmatrix} \leq 0, \tag{61}$$

$$\begin{bmatrix} -\urcorner_{3-q} \tilde{Q}_{k(3-q)} & X_{k(3-q)} \\ * & \varepsilon_{kq}^2 \tilde{Q}_{kq} - 2\varepsilon_{kq} X_{kq} \end{bmatrix} \leq 0, \tag{62}$$

$$\begin{bmatrix} -\urcorner_{3-q} \tilde{R}_{k(3-q)} & X_{k(3-q)} \\ * & \varphi_{kq}^2 \tilde{R}_{kq} - 2\varphi_{kq} X_{kq} \end{bmatrix} \leq 0, \tag{63}$$

$$\begin{bmatrix} -\urcorner_{3-q} \tilde{Z}_{k(3-q)} & X_{k(3-q)} \\ * & \varsigma_{kq}^2 \tilde{Z}_{kq} - 2\varsigma_{kq} X_{kq} \end{bmatrix} \leq 0, \tag{64}$$

$$\begin{bmatrix} -X_{1q} & X_{1q} C_1^T \\ * & -\Lambda_4^{-1} \end{bmatrix} \leq 0, \tag{65}$$

where

$$\Phi^1 = \begin{bmatrix} \Phi^1_{13\times 13} & \sqrt{h}\Phi_1^1 & \sqrt{\tau_2}\Phi_2^1 & \Phi_3^1 & \Phi_4^1 \\ * & \Phi_2^1 & 0 & 0 & 0 \\ * & * & \Phi_3^1 & 0 & 0 \\ * & * & * & -I & 0 \\ * & * & * & * & -I \end{bmatrix},$$

$$\Phi^2 = \begin{bmatrix} \Phi^2_{11\times 11} & \Phi_1^2 & \Phi_2^2 & \Phi_4^2 \\ * & \Phi_2^2 & 0 & 0 \\ * & * & \Phi_3^2 & 0 \\ * & * & * & -I \end{bmatrix},$$

$$\begin{aligned}
\Phi^q_{1,1} &= A_1X_{1q} + X_{1q}^T A_1^T + \tilde{Q}_{1q} - 4e^{2(-1)^q\delta_q h}\tilde{Z}_{1q} \\
&\quad - 2(-1)^q\delta_q X_{1q}, \\
\Phi^q_{1,2} &= -2e^{2(-1)^q\delta_q h}\tilde{Z}_{1q}, \\
\Phi^q_{1,4} &= 6e^{2(-1)^q\delta_q h}\tilde{Z}_{1q}, \\
\Phi^q_{1,6} &= B_1C_2X_{2q}, \\
\Phi^1_{1,13} &= B_1D_2 - X_{11}C_1^T\Lambda_2, \\
\Phi^2_{1,11} &= B_1D_2 - X_{12}C_1^T\Lambda_2, \\
\Phi^1_{2,2} &= -8e^{-2\delta_1 h}\tilde{Z}_{11} + \vartheta\tilde{\mathfrak{H}}, \\
\Phi^2_{2,2} &= -8e^{2\delta_2 h}\tilde{Z}_{12}, \\
\Phi^q_{2,3} &= -2e^{2(-1)^q\delta_q h}\tilde{Z}_{1q}, \\
\Phi^q_{2,4} &= 6e^{2(-1)^q\delta_q h}\tilde{Z}_{1q}, \\
\Phi^q_{2,5} &= 6e^{2(-1)^q\delta_q h}\tilde{Z}_{1q}, \\
\Phi^1_{2,6} &= \tilde{\mathbf{B}}_1^T, \\
\Phi^1_{2,11} &= \vartheta\tilde{\mathfrak{H}}, \\
\Phi^q_{3,3} &= -e^{2(-1)^q\delta_q h}(\tilde{Q}_{1q} + 4\tilde{Z}_{1q}), \\
\Phi^q_{3,5} &= 6e^{2(-1)^q\delta_q h}\tilde{Z}_{1q}, \\
\Phi^q_{4,4} &= -12e^{2(-1)^q\delta_q h}\tilde{Z}_{1q}, \\
\Phi^q_{5,5} &= -12e^{2(-1)^q\delta_q h}\tilde{Z}_{1q}, \\
\Phi^1_{6,6} &= A_2X_{21} + X_{21}^TA_2^T + 2\hat{\mathcal{B}}_1 \\
&\quad + \tilde{Q}_{21} + \tilde{R}_{1q} + \tau_2\tilde{R}_{21} + 2\delta_1E^TX_{21} \\
&\quad - 4e^{-2\delta_1\tau_2}E^T\tilde{Z}_{21}E, \\
\Phi^2_{6,6} &= A_2X_{22} + X_{22}^TA_2^T + \tilde{Q}_{22} + \tilde{R}_{12} + \tau_2\tilde{R}_{22} \\
&\quad - 2\delta_2E^TX_{22} - 4e^{2\delta_2\tau_2}E^T\tilde{Z}_{22}E, \\
\Phi^q_{6,7} &= A_3X_{2q} - 2e^{2(-1)^q\delta_q\tau_2}E^T\tilde{Z}_{2q}E, \\
\Phi^q_{6,9} &= 6e^{2(-1)^q\delta_q\tau_2}E^T\tilde{Z}_{2q}E, \\
\Phi^1_{6,11} &= \tilde{\mathbf{B}}_1, \\
\Phi^1_{6,12} &= -\bar{\mathcal{B}}_1, \\
\Phi^1_{6,13} &= B_3, \\
\Phi^2_{6,11} &= B_3, \\
\Phi^q_{7,7} &= -(1-\nu)e^{2(-1)^q\delta_q\tau_2}\tilde{R}_{1q} - 8e^{2(-1)^q\delta_q\tau_2}E^T\tilde{Z}_{2q}E, \\
\Phi^q_{7,8} &= -2e^{2(-1)^q\delta_q\tau_2}E^T\tilde{Z}_{2q}E, \\
\Phi^q_{7,9} &= 6e^{2(-1)^q\delta_q\tau_2}E^T\tilde{Z}_{2q}E, \\
\Phi^q_{7,10} &= 6e^{2(-1)^q\delta_q\tau_2}E^T\tilde{Z}_{2q}E, \\
\Phi^q_{8,8} &= -e^{2(-1)^q\delta_q\tau_2}(\tilde{Q}_{2q} + 4E^T\tilde{Z}_{2q}E), \\
\Phi^q_{8,10} &= 6e^{2(-1)^q\delta_q\tau_2}E^T\tilde{Z}_{2q}E, \\
\Phi^q_{9,9} &= -12e^{2(-1)^q\delta_q\tau_2}E^T\tilde{Z}_{2q}E - \frac{1}{\tau_2}\tilde{R}_{2q}, \\
\Phi^q_{10,10} &= -12e^{2(-1)^q\delta_q\tau_2}E^T\tilde{Z}_{2q}E \\
&\quad - \frac{1}{\tau_2}\tilde{R}_{2q}, \\
\Phi^1_{11,11} &= -\tilde{\mathfrak{H}}, \\
\Phi^1_{12,12} &= -I, \\
\Phi^1_{13,13} &= -2D_1^T\Lambda_2 - \Lambda_3, \\
\Phi^2_{11,11} &= -2D_1^T\Lambda_2 - \Lambda_3, \\
\Phi^1_2 &= \urcorner_{11}^2\tilde{Z}_{11} - 2\urcorner_{11}X_{11}, \\
\Phi^1_3 &= \urcorner_{21}^2\tilde{Z}_{21} - 2\urcorner_{21}X_{21}, \\
\Phi^2_2 &= \urcorner_{12}^2\tilde{Z}_{12} - 2\urcorner_{12}X_{12}, \\
\Phi^2_3 &= \urcorner_{22}^2\tilde{Z}_{22} - 2\urcorner_{22}X_{22}, \\
\Phi^1_1 &= \\
&\quad \begin{bmatrix} A_1X_{11} & 0_{1\times 4} & B_1C_2X_{21} & 0_{1\times 6} & B_1D_2 \end{bmatrix}^T, \\
\Phi^1_2 &= \\
&\quad \begin{bmatrix} 0 & \tilde{\mathbf{B}}_1 & 0_{1\times 3} & X_{21}A_2 + \hat{\mathcal{B}}_1 & X_{21}A_3 & 0_{1\times 3} & \tilde{\mathbf{B}}_1 & -\bar{\mathcal{B}}_1 & B_3 \end{bmatrix}^T, \\
\Phi^1_3 &= \\
&\quad \begin{bmatrix} 0 & \sqrt{\epsilon}\mathfrak{I}Y_1 & 0_{1\times 3} & \sqrt{\epsilon}Y_2 & 0_{1\times 4} & \sqrt{\epsilon}\mathfrak{I}Y_1 & 0 & 0 \end{bmatrix}^T, \\
\Phi^1_4 &= \begin{bmatrix} \hat{\Lambda}_1C_1X_{11} & 0_{1\times 11} & \hat{\Lambda}_1D_1 \end{bmatrix}^T, \\
\Phi^2_1 &= \begin{bmatrix} X_{12}A_1 & 0_{1\times 4} & X_{12}B_1C_2 & 0_{1\times 4} & B_1D_2 \end{bmatrix}^T,
\end{aligned}$$

$$\Phi_2^2 = \begin{bmatrix} 0_{1\times5} & X_{22}A_2 & X_{22}A_3 & 0_{1\times3} & B_3 \end{bmatrix}^T,$$
$$\Phi_4^2 = \begin{bmatrix} \hat{\Lambda}_1 C_1 X_{12} & 0_{1\times9} & \hat{\Lambda}_1 D_1 \end{bmatrix}^T, \text{and } \tilde{\mathbf{B}}_1 = B_2(I - \bar{\aleph})Y_1.$$

Proof: First, we define $X_{kq} = P_{kq}^{-1}$, $\mathfrak{S}_1 = \text{diag}\{\mathfrak{S}_{11}, \mathfrak{S}_{21}, X_{11}, I, I, X_{11}, X_{21}, X_{11}, I\}$, $\mathfrak{S}_2 = \text{diag}\{\mathfrak{S}_{12}, \mathfrak{S}_{22}, I, X_{12}, X_{22}, X_{12}\}$, $\mathfrak{S}_{kq} = \text{diag}\{X_{kq}, X_{kq}, X_{kq}, X_{kq}, X_{kq}, X_{kq}\}$. Then, we take the pre- and post-multiply of Ω^q in (26) with $\mathfrak{S}_q$.

Next, we define $\tilde{\Delta}_{kq} = X_{kq}\Delta_{kq}X_{kq}$, $\Delta \in \{Q, R, Z\}$, $\tilde{\mathfrak{H}} = X_{11}\mathfrak{H}X_{11}$, $Y_1 = K_1X_{11}$, $Y_2 = K_2X_{21}$ with $(k, q = 1, 2)$. By using the connections $Z_{kq} = X_{kq}^{-1}\tilde{Z}_{kq}X_{kq}^{-1}$, $Z_{kq}^{-1} = X_{kq}\tilde{Z}_{kq}^{-1}X_{kq} \geq 2F_{kq}X_{kq} - F_{kq}^2\tilde{Z}_{kq}$, we obtain $\Phi^q < 0$ to ensure that $\Omega^q < 0$ is satisfied. In addition, pre- and post-multiplying (27) and (28) by X_{12} and X_{11}, respectively. Applying Schur Complement Lemma, we have (60) and (61) are equal to (27) and (28), respectively. By employing the similar approach, it is obvious that LMIs (29) and (30) tends to (62)-(64) and (65), respectively. This completes the proof of this theorem.

Remark 10: This work mainly focuses on the problem of dissipation, time-varying actuator faults, and DoS attacks. The idea of extended dissipative is presented in Definition 3 and includes some well-known performance lists as special cases where the weight matrices are

- $L_2 - L_\infty$ performance: $\Lambda_1 = 0$, $\Lambda_2 = 0$, $\Lambda_3 = \gamma^2 I$, $\Lambda_4 = I$.
- H_∞ performance: $\Lambda_1 = -I$, $\Lambda_2 = 0$, $\Lambda_3 = \gamma^2 I$, $\Lambda_4 = 0$.
- Passivity performance: $\Lambda_1 = 0$, $\Lambda_2 = I$, $\Lambda_3 = \gamma I$, $\Lambda_4 = 0$.
- $(\mathcal{Q}, \mathcal{S}, \mathcal{R})$-dissipativity performance: $\Lambda_1 = \mathcal{Q}$, $\Lambda_2 = \mathcal{S}$, $\Lambda_3 = \mathcal{R} - \beta I$, $\Lambda_4 = 0$.

Remark 11: The choice of the LKF plays crucial role in stability analysis for time-delay systems. Apart from the functional choice, the significance of conservatism is determined by how to bound some cross terms that appeared when calculating LKF differentiation. From this perspective, Jensen's and Wirtinger-based integral inequalities are used by researchers to obtain a more accurate lower bound of these cross terms. Moreover, Wirtinger-based integral inequality approach produces less conservative results than Jensen's integral inequality approach, which is presented in [29] and theoretically proven.

Remark 12: It should be noted that the proposed AETM is only considered in the absence of DoS attack. In addition, the proposed scheme is implemented in a periodic sampling context. Thus, the minimum release intervals between two consecutive transmission instants of considered triggering mechanism (9) is one sampling period h. As a result, the Zeno behavior can be ruled out completely. Besides, the resilient ET mechanism does not transmit data during the active period of DoS attacks, thus attack-induced data dropouts are avoided.

Remark 13: In this paper, the output of the saturation function (4) can be divided into linear and nonlinear terms.

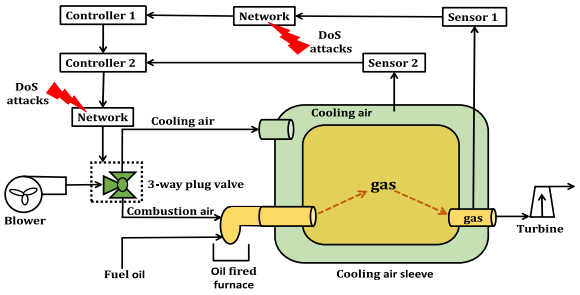

FIGURE 2. Structure diagram of SNCCS for a power plant boiler-turbine system.

In particular, this nonlinear term adds the dimension of LMI condition. The computational complexity of the proposed method will be increased due to the large size of LMI condition. With the help of standard optimization software, the obtained conditions in Theorems 8 and 9 can then be easily solved.

Remark 14: It should be pointed out that the LMI method was used to achieve the desired results in this study. Moreover, a large number of decision variables in the LMI leads to computational problems for the main outcomes. In this present study, our objective is to develop a new stability criterion that is less conservative and contains fewer decision variables. In order to accomplish this, we used the Wirtinger-based integral inequality and Jensen's integral inequality to reduce conservatism without introducing new variables in the main results.

IV. SIMULATION EXAMPLE

In this example, we borrow a power plant gas turbine system [17] to illustrate the effectiveness of the theoretical results. The operating principle of the SNCCS is displayed in FIGURE 2, where the safety and reliability of the turbine largely depends on the temperature of the superheated gas. When the gas generation is carried out, the blower increases the velocity of the air and directs it to a 3-way plug valve, which in turn directs air to two different sides. First, the air is used to cool the superheated gas. Then, it acts as a combustion enhancer in the combustion of fuel oil to produce the superheated gas. In order to generate superheated gas with an appropriate temperature, the SNCCS is designed for the gas turbine system. In this design, the gas outlet temperature is determined by the primary sensor **Sensor 1** and the cooling air temperature is determined by the secondary sensor **Sensor 2**.

The data from the primary sensor **Sensor 1** is transmitted to the primary controller **Controller 1** through a real-time network. The output of the secondary controller **Controller 2** controls the 3-way control valve to modulate the outlet air over two directions. The output signals from the primary controller **Controller 1** and the secondary sensor **Sensor 2** are passed to secondary controller **Controller 2**, which controls the three-way control valve to regulate the air outlets on both

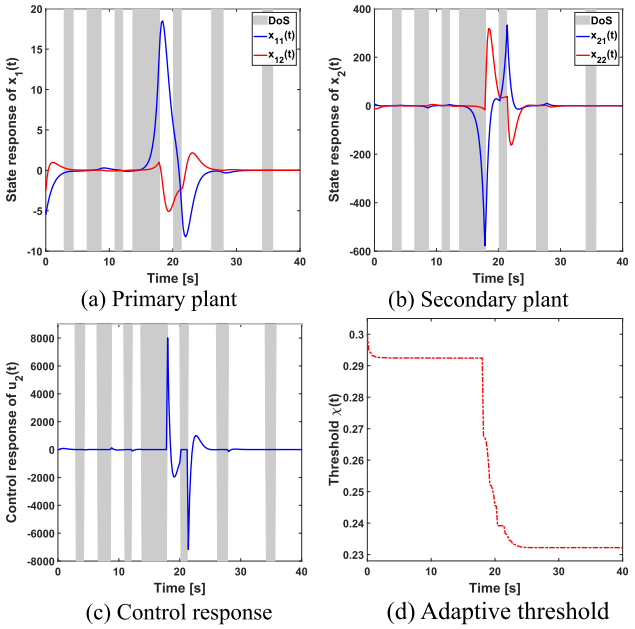

(a) Primary plant (b) Secondary plant (c) Control response (d) Adaptive threshold

FIGURE 3. State, control, and threshold responses for considered system under H_∞ controller.

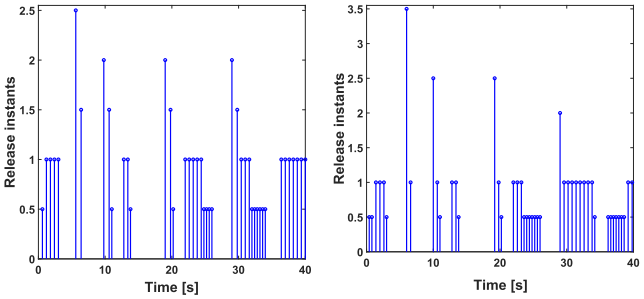

(a) Adaptive ET scheme (b) Traditional ET scheme

FIGURE 4. Simulation results of release instant and intervals under H_∞ controller.

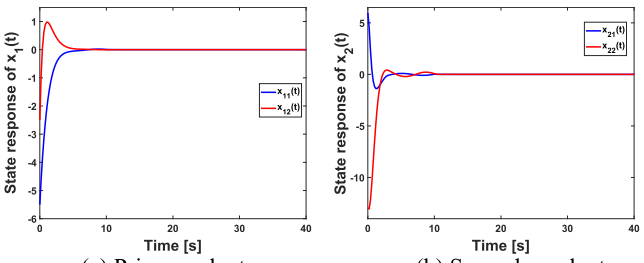

(a) Primary plant (b) Secondary plant

FIGURE 5. State and control responses for considered system without DoS attacks.

sides to ensure an suitable gas temperature. In the following, the parameter values of the primary and secondary plants of the SNCCS are taken from [17] such that

$$\dot{x}_1(t) = \begin{bmatrix} -1 & 0 \\ -1 & -2 \end{bmatrix} x_1(t) + \begin{bmatrix} 0.2 \\ 0.1 \end{bmatrix} y_2(t),$$
$$y_1(t) = \begin{bmatrix} 0 & 0.1 \end{bmatrix} x_1(t) + 0.2w(t),$$

$$\begin{bmatrix} 1 & 0 \\ 0 & 0 \end{bmatrix} \dot{x}_2(t) = \begin{bmatrix} 1.3 & 1 \\ 0.2 & 0 \end{bmatrix} x_2(t) + \begin{bmatrix} 0.2 & 0.1 \\ 0.2 & 1 \end{bmatrix} x_2(t - \tau(t)) + \begin{bmatrix} 0.2 \\ 1 \end{bmatrix} u_2(t) + \begin{bmatrix} -0.4 \\ 0.1 \end{bmatrix} w(t),$$
$$y_2(t) = \begin{bmatrix} -0.3 & 0.1 \end{bmatrix} x_2(t) + 0.1w(t).$$

The other parameters are as follows: $\delta_1 = 0.7$, $\delta_2 = 2$, $\urcorner_1 = 1.5$, $\urcorner_2 = 1.5$, $F_{1q} = 8$, $F_{2q} = 8$, $\varepsilon_{1q} = 8$, $\varepsilon_{2q} = 8$, $\varphi_{1q} = 8$, $\varphi_{2q} = 8$, $\varsigma_{1q} = 8$, $\varsigma_{2q} = 8$, $\vartheta = 5$, $\omega_G = 3.5s$, $\omega_D = 5s$, and the fault model is adopted as $\aleph(t) = 0.85 + 0.05\sin(5t)$. Therefore, Definition 3 includes $L_2 - L_\infty$, H_∞, mixed H_∞ and passivity, passivity, and also $(\mathcal{Q}, \mathcal{S}, \mathcal{R})$-dissipativity performances as special cases. We are able to discuss all the above performances in the following cases when the weighting parameters Λ_1, Λ_2, Λ_3, and Λ_4 are set as indicated in Remark 10. For the simulation, we choose $\begin{bmatrix} -5.5 & -2.5 \end{bmatrix}^T$ and $\begin{bmatrix} 6 & -12.96 \end{bmatrix}^T$ as initial conditions for Σ_1 and Σ_2, respectively. The external disturbance is taken as $w(t) = \begin{cases} \sin(t), & 0 < t \leq 10, \\ 0, & \text{otherwise} \end{cases}$.

H_∞ performance: Let $\Lambda_1 = -I$, $\Lambda_2 = 0$, $\Lambda_3 = \gamma^2 I$, $\Lambda_4 = 0$, $h = 0.2s$, and $\tau_2 = 0.2s$. By using the above parameters and calculating the feasibility issue for the LMIs in Theorem 9 with the MATLAB LMI Toolbox, we obtain the primary and secondary controller gain matrices, and the triggering parameter as follows:

$$K_1 = \begin{bmatrix} 0.0476 & 0.0239 \end{bmatrix},$$
$$K_2 = \begin{bmatrix} -20.6146 & -8.2811 \end{bmatrix},$$
$$\text{and} \quad \mathfrak{H} = \begin{bmatrix} 0.8098 & 0.1660 \\ 0.1660 & 2.4320 \end{bmatrix}.$$

By using the controller gains and initial conditions determined above, the primary and secondary state trajectories of the system (24) are plotted in FIGURES 3 (a) and (b), respectively, where the shaded regions represent the time intervals of the aperiodic DoS attacks. The control response of $u_2(t)$ is shown in FIGURE 3 (c). Our proposed control strategy can eliminate the effects of aperiodic DoS attacks and reduce the communication burden under H_∞ performance, which shows the effectiveness of the proposed control strategy. The adaptive threshold response of $\chi(t)$ is depicted in FIGURE 3 (d), and the corresponding relationship between triggering instants and release intervals is given in FIGURE 4 (a). The releasing time instants and intervals according to the traditional ET scheme are shown in FIGURE 4 (b).

In the H_∞ case, we observe that 42 and 46 packets are transmitted to the controller with the proposed AETM and the traditional ET scheme, respectively. The average transmission time for the AETM and the traditional ET scheme

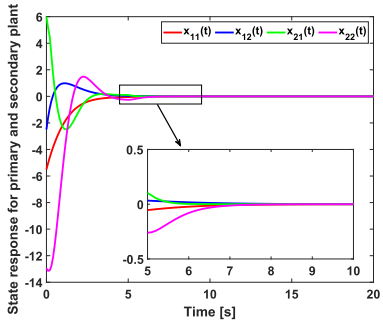

(a) State response with AETM under H_∞ case

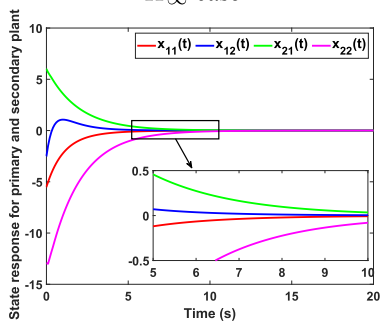

(b) State response of Figure 4 in [17]

FIGURE 6. State response of SNCCSs for heating furnace.

TABLE 1. Calculated number of transmitted data for various methods under H_∞ case.

Method	Number of transmission
Traditional ET scheme	46
Proposed method	42

TABLE 2. Calculated $\gamma_{\min}$ for different values of τ_2 with $h = 0.2$ under H_∞ case.

τ_2	0.01	0.05	0.1	0.15	0.2
Theorem 3.2	0.2739	0.2883	0.3047	0.3214	0.3414

are 0.9524 and 0.8696, respectively. From TABLE 1, it can be seen that the number of transmitted data packets with the proposed AETM is less than that with the traditional ET scheme. TABLE 2 displays the $\gamma_{\min}$ of various values of τ_2 with $h = 0.2s$, where the delay of the secondary state increases and the associated minimum performance index $\gamma_{\min}$ also increases.

In the absence of aperiodic DoS attacks, the trajectories of the primary state and secondary state are presented in FIGURES 5 (a) and (b), respectively. Moreover, it can be seen in FIGURES 3 and 5 that the trajectories of the primary and secondary system states quickly approach zero when there are no aperiodic DoS attacks under H_∞ performance.

For comparison, we consider the external disturbance $w(t)$ is $\begin{cases} \sin(t), & 0 < t \leq 5, \\ 0, & \text{otherwise} \end{cases}$ and the time period $t \in (0, 20]$, the primary and secondary state responses are plotted in FIGURE 6 (a) under proposed method without DoS attacks, while

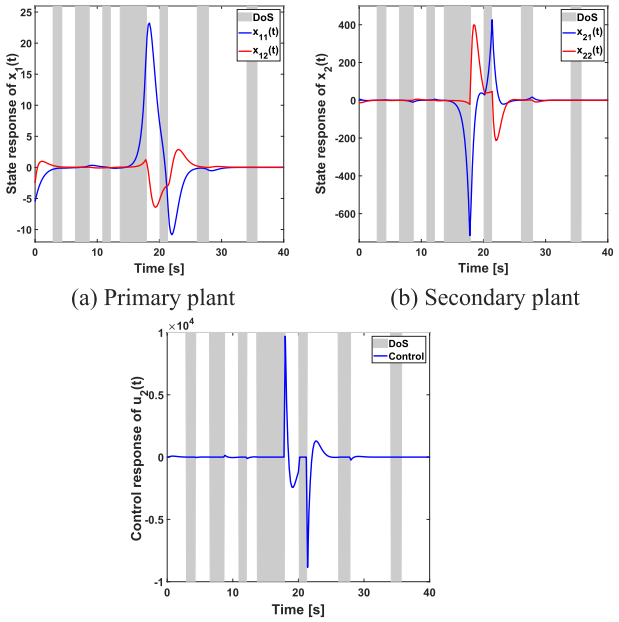

(a) Primary plant (b) Secondary plant

(c) Control response

FIGURE 7. State and control responses for considered system under dissipative controller.

the H_∞ controller method in [17] is shown in FIGURE 6 (b). According to the FIGURE 6, it is concluded that the trajectories of the system states converge to the equilibrium point faster under AETM without DoS attacks than the H_∞ controller in [17], which shows the superiority of the proposed controller scheme. The simulation results clearly show that the proposed method is feasible and effectively removed the attack signals. Also, the proposed AETM reduced the communication bandwidth.

$(\mathcal{Q}, \mathcal{S}, \mathcal{R})$ **- dissipative performance:** We consider $\Lambda_1 = \mathcal{Q}$, $\Lambda_2 = \mathcal{S}$, $\Lambda_3 = \mathcal{R} - \beta I$, $\Lambda_4 = 0$, $h = 0.2s$, and $\tau_2 = 0.2s$ with $\mathcal{Q} = -1$, $\mathcal{S} = 0.3$, $\mathcal{R} = 0.5$ and $\beta = 0.0001$. By solving conditions (25), (59)-(65), and using the above parameters found to be feasible, the following primary and secondary controller gains and triggering parameter are obtained as

$$K_1 = \begin{bmatrix} 0.0627 & 0.0185 \end{bmatrix},$$
$$K_2 = \begin{bmatrix} -19.8495 & -8.1371 \end{bmatrix},$$
$$\text{and} \quad \mathfrak{H} = \begin{bmatrix} 0.6207 & 0.1429 \\ 0.1429 & 2.1786 \end{bmatrix}.$$

Under the above primary and secondary gain matrices, exogenous disturbance, and initial condition, the state responses of the primary plant (66) are plotted in FIGURE 7 (a). FIGURE 7 (b) shows the secondary state response of the system (66). The control response of the secondary control input is presented in FIGURE 7 (c), where the shaded areas represent the time intervals of the aperiodic DoS attacks. Our proposed AETM can remove the consequences of aperiodic DoS attacks and also reduce the communication burden under $(\mathcal{Q}, \mathcal{S}, \mathcal{R})$ - dissipative. The adaptive threshold response of

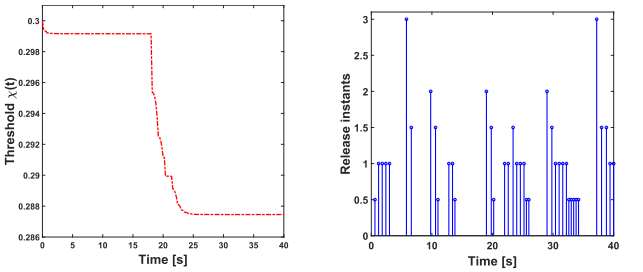

(a) Adaptive threshold (b) Release instants and intervals

FIGURE 8. Simulation results of $\chi(t)$ and the corresponding release instant and intervals under dissipative controller.

TABLE 3. Maximum allowable upper bound of τ_2 with $h = 0.2$ and $\gamma = 0.5$ for various cases.

Cases	τ_2
H_∞	0.4350
$L_2 - L_\infty$	0.4542
Passivity	0.5254
$(\mathcal{Q}, \mathcal{S}, \mathcal{R})$-dissipative	0.4992

$\chi(t)$ is plotted in FIGURE 8 (a). Moreover, the release time instants and release intervals are displayed in FIGURE 8 (b). It is noted that the 37 packets are transmitted to the controller under proposed AETM. Furthermore, the maximum allowable upper bound for τ_2 is given for various cases, such as H_∞, $L_2 - L_\infty$, passivity, and $(\mathcal{Q}, \mathcal{S}, \mathcal{R})$ - dissipative in TABLE 3, where $h = 0.2s$. The simulation results show that the system trajectories converge well in the different cases even under DoS attacks. The transmission frequency is also significantly reduced by AETM.

V. CONCLUSION

The problem of resilient adaptive ET control for SNCCSs with aperiodic DoS attacks was investigated. In particular, a switched strategy was developed to describe aperiodic DoS attacks. The AETM was introduced to reduce the data transmission in SNCCSs while mitigating the aperiodic DoS attacks. Using the Wirtinger-based integral inequality and the LKF approach, sufficient conditions for the exponential admissibility of SNCCSs with a prescribed extended dissipative performance under AETM have been derived in terms of LMIs. Finally, a simulation example was used to show the efficacy of the developed method. In future work, we will investigate the proposed method for neural-network-based control design [11] and filtering-based control design [25] with DoS attacks.

REFERENCES

[1] Z. Gu, T. Zhang, F. Yang, H. Zhao, and M. Shen, "A novel event-triggered mechanism for networked cascade control system with stochastic nonlinearities and actuator failures," *J. Franklin Inst.*, vol. 356, no. 4, pp. 1955–1974, Mar. 2019.

[2] C. Wu and X. Zhao, "Quantized dynamic output feedback control and L_2-gain analysis for networked control systems: A hybrid approach," *IEEE Trans. Netw. Sci. Eng.*, vol. 8, no. 1, pp. 575–587, Mar. 2021.

[3] H. Congzhi, B. Yan, and L. Xiangjie, "H-infinity state feedback control for a class of networked cascade control systems with uncertain delay," *IEEE Trans. Ind. Informat.*, vol. 6, no. 1, pp. 62–72, Feb. 2010.

[4] J. Liu, Y. Gu, X. Xie, D. Yue, and J. H. Park, "Hybrid-driven-based $\mathcal{H}_\infty$ control for networked cascade control systems with actuator saturations and stochastic cyber attacks," *IEEE Trans. Syst., Man Cybern., Syst.*, vol. 49, no. 12, pp. 2452–2463, Dec. 2019.

[5] F. Fang, H. Ding, Y. Liu, and J. H. Park, "Fault tolerant sampled-data $\mathcal{H}_\infty$ control for networked control systems with probabilistic time-varying delay," *Inf. Sci.*, vol. 544, pp. 395–414, Jan. 2021.

[6] M. Palmisano, M. Steinberger, and M. Horn, "Optimal finite-horizon control for networked control systems in the presence of random delays and packet losses," *IEEE Control Syst. Lett.*, vol. 5, no. 1, pp. 271–276, Jan. 2021.

[7] H. Sun, J. Sun, and J. Chen, "Analysis and synthesis of networked control systems with random network-induced delays and sampling intervals," *Automatica*, vol. 125, Mar. 2021, Art. no. 109385.

[8] S. Feng and P. Tesi, "Networked control systems under denial-of-service: Co-located vs. remote architectures," *Syst. Control Lett.*, vol. 108, pp. 40–47, Oct. 2017.

[9] C. D. Persis and P. Tesi, "Networked control of nonlinear systems under denial-of-service," *Syst. Control Lett.*, vol. 96, pp. 124–131, Oct. 2016.

[10] A. Cetinkaya, H. Ishii, and T. Hayakawa, "Event-triggered output feedback control resilient against jamming attacks and random packet losses," *IFAC PapersOnLine*, vol. 48, no. 22, pp. 270–275, 2015.

[11] H. Song, D. Ding, H. Dong, and X. Yi, "Distributed filtering based on Cauchy-kernel-based maximum correntropy subject to randomly occurring cyber-attacks," *Automatica*, vol. 135, Jan. 2022, Art. no. 110004.

[12] C. De Persis and P. Tesi, "Input-to-state stabilizing control under denial-of-service," *IEEE Trans. Autom. Control*, vol. 60, no. 11, pp. 2930–2944, Nov. 2015.

[13] N. Zhao, P. Shi, W. Xing, and C. P. Lim, "Event-triggered control for networked systems under denial of service attacks and applications," *IEEE Trans. Circuits Syst. I, Reg. Papers*, vol. 69, no. 2, pp. 811–820, Feb. 2022.

[14] D. Liu and D. Ye, "Pinning-observer-based secure synchronization control for complex dynamical networks subject to DoS attacks," *IEEE Trans. Circuits Syst. I, Reg. Papers*, vol. 67, no. 12, pp. 5394–5404, Dec. 2020.

[15] N. Zhao, P. Shi, and W. Xing, "Dynamic event-triggered approach for networked control systems under denial of service attacks," *Int. J. Robust Nonlinear Control*, vol. 31, no. 5, pp. 1774–1795, Mar. 2021.

[16] Y. Deng, X. Yin, and S. Hu, "Event-triggered predictive control for networked control systems with DoS attacks," *Inf. Sci.*, vol. 542, pp. 71–91, Jan. 2021.

[17] Z. Du, D. Yue, and S. Hu, "H-infinity stabilization for singular networked cascade control systems with state delay and disturbance," *IEEE Trans. Ind. Informat.*, vol. 10, no. 2, pp. 882–894, May 2014.

[18] Z. Du, W. Li, J. Li, and X. Yang, "Event-triggered H-infinity control for continuous-time singular networked cascade control systems with state delay," *IEEE Access*, vol. 8, pp. 2760–2771, 2020.

[19] W. Xing, P. Shi, R. K. Agarwal, and L. Li, "Robust H_∞ pinning synchronization for complex networks with event-triggered communication scheme," *IEEE Trans. Circuits Syst. I, Reg. Papers*, vol. 67, no. 12, pp. 5233–5245, Dec. 2020.

[20] Y. Xu, M. Fang, Y. Pan, K. Shi, and Z. Wu, "Event-triggered output synchronization for nonhomogeneous agent systems with periodic denial-of-service attacks," *Int. J. Robust Nonlinear Control*, vol. 31, no. 6, pp. 1851–1865, Apr. 2021.

[21] H. Sun, C. Peng, W. Zhang, T. Yang, and Z. Wang, "Security-based resilient event-triggered control of networked control systems under denial of service attacks," *J. Franklin Inst.*, vol. 356, no. 17, pp. 10277–10295, Nov. 2019.

[22] J. Zhang, P. Chen, and D. Peng, "A novel adaptive event-triggered communication scheme for networked control systems with nonlinearities," in *Proc. Comput. Intell. Netw. Syst. Appl.*, vol. 462, Sep. 2014, pp. 468–477.

[23] M. Sathishkumar and Y.-C. Liu, "Resilient annular finite-time bounded and adaptive event-triggered control for networked switched systems with deception attacks," *IEEE Access*, vol. 9, pp. 92288–92299, 2021.

[24] W. Qi, G. Zong, and W. X. Zheng, "Adaptive event-triggered SMC for stochastic switching systems with semi-Markov process and application to boost converter circuit model," *IEEE Trans. Circuits Syst. I, Reg. Papers*, vol. 68, no. 2, pp. 786–796, Feb. 2021.

[25] X. Wang, D. Ding, X. Ge, and Q. Han, "Neural-network-based control for discrete-time nonlinear systems with denial-of-service attack: The adaptive event-triggered case," *Int. J. Robust Nonlinear Control*, vol. 32, no. 5, pp. 2760–2779, Mar. 2022.
[26] B. Zhang, W. X. Zheng, and S. Xu, "Filtering of Markovian jump delay systems based on a new performance index," *IEEE Trans. Circuits Syst. I, Reg. Papers*, vol. 60, no. 5, pp. 1250–1263, May 2013.
[27] X. Liu, F. Deng, P. Zeng, X. Gao, and X. Zhao, "Sampled-data resilient control for hybrid nonlinear stochastic systems under periodic DoS attacks," *IEEE Access*, vol. 9, pp. 49881–49889, 2021.
[28] S. Murugesan and Y.-C. Liu, "Resilient memory event-triggered finite-time bounded for networked control systems with multiple cyber-attacks," in *Proc. Amer. Control Conf. (ACC)*, May 2021, pp. 2713–2719.
[29] A. Seuret and F. Gouaisbaut, "Wirtinger-based integral inequality: Application to time-delay systems," *Automatica*, vol. 49, no. 9, pp. 2860–2866, Sep. 2013.

M. SATHISHKUMAR (Member, IEEE) received the B.Sc. degree in mathematics from the Government Arts College, Coimbatore, India, in 2009, the M.Sc. and M.Phil. degrees in mathematics from the Sri Ramakrishna Mission Vidyalaya College of Arts and Science affiliated to Bharathiar University, India, in 2011 and 2013, respectively, and the Ph.D. degree in mathematics from Anna University, Chennai, India, in 2018. He was an Assistant Professor with the Department of Mathematics, Christ the King Engineering College, Coimbatore, India, from 2013 to 2014. He is currently a Postdoctoral Research Fellow with the Department of Mechanical Engineering, National Cheng Kung University, Tainan, Taiwan. His current research interests include networked control systems and its security control, multi-agent systems, and time-delay systems.

YEN-CHEN LIU (Senior Member, IEEE) received the B.S. and M.S. degrees in mechanical engineering from National Chiao Tung University, Hsinchu, Taiwan, in 2003 and 2005, respectively, and the Ph.D. degree in mechanical engineering from the University of Maryland, College Park, MD, USA, in 2012.

He is currently a Professor with the Department of Mechanical Engineering, National Cheng Kung University, Tainan, Taiwan. His research interests include vehicle dynamic control, networked robotic systems, aerial robotics, multi-robot systems, mobile robot networks, and human–robot interaction.

Dr. Liu was a recipient of the Outstanding Young Faculty, Chinese Society of Mechanical Engineering (CSME), Taiwan, in 2015; the Ta-You Wu Memorial Award, Ministry of Science and Technology (MOST), Taiwan, in 2016; the Outstanding Young Robotics Award, Robotics Society of Taiwan (RST), Taiwan, in 2017; the Kwoh-Ting Li Researcher Award, National Cheng Kung University, in 2018; and the Young Scholar Fellowship-Columbus Program, MOST, in 2019.